Received Date : 15-Aug-2016

Revised Date : 15-Sep-2016

Accepted Date : 22-Sep-2016

Article type : Regular Paper

"This is the peer reviewed version of the following article: Onetti, Y., Dantas, A. P., Pérez, B., McNeish, A. J., Vila, E. and Jiménez-Altayó, F. (2016), Peroxynitrite formed during a transient episode of brain ischaemia increases endothelium-derived hyperpolarization-type dilations in thromboxane/prostaglandin receptor-stimulated rat cerebral arteries. Acta Physiol. which has been published in final form at http://dx.doi.org/10.1111/apha.12809. This article may be used for non-commercial purposes in accordance with Wiley Terms and Conditions for Self-Archiving."

Peroxynitrite formed during a transient episode of brain ischemia increases endothelium-derived hyperpolarization-type dilations in thromboxane/prostaglandin receptor-stimulated rat cerebral arteries

Yara Onetti[1], Ana P Dantas[2], Belen Pérez[1], Alister J McNeish[3], Elisabet Vila[1], Francesc Jiménez-Altayó[1]

[1]Departament de Farmacologia, de Terapèutica i de Toxicologia, Institut de Neurociències, Facultat de Medicina, Universitat Autònoma de Barcelona, Bellaterra, Spain. [2]Institut Clínic Cardiovascular, Institut d'Investigacions Biomèdiques August Pi i Sunyer (IDIBAPS), Barcelona, Spain. [3]Reading School of Pharmacy, University of Reading, Reading, Berkshire, UK.

Correspondence: Dr F Jiménez-Altayó, Departament de Farmacologia, de Terapèutica i de Toxicologia, Facultat de Medicina, Universitat Autònoma de Barcelona, 08193 Bellaterra (Cerdanyola del Vallès), Spain. E-mail: francesc.jimenez@uab.cat, Tel: (+34) 93 581 1952; Fax: (+34) 93 581 1953

This article has been accepted for publication and undergone full peer review but has not been through the copyediting, typesetting, pagination and proofreading process, which may lead to differences between this version and the Version of Record. Please cite this article as doi: 10.1111/apha.12809

This article is protected by copyright. All rights reserved.

Accepted Article

Short title: Peroxynitrite dilates cerebral arteries

Accepted Article

Abstract

AIM: Increased thromboxane A_2 and peroxynitrite are hallmarks of cerebral ischemia/reperfusion (I/R). Stimulation of thromboxane/prostaglandin receptors (TP) attenuates endothelium-derived hyperpolarization (EDH). We investigated whether EDH-type middle cerebral artery (MCA) relaxations following TP stimulation are altered after I/R and the influence of peroxynitrite.

METHODS: Vascular function was determined by wire myography after TP stimulation with the thromboxane A_2 mimetic 9,11-Dideoxy-9α,11α-methano-epoxy prostaglandin F2α (U46619) in MCA of Sprague-Dawley rats subjected to MCA occlusion (90 min)/reperfusion (24 h) or sham operation, and in non-operated (control) rats. Some rats were treated with saline or the peroxynitrite decomposition catalyst 5,10,15,20-tetrakis(4-sulfonatophenyl)prophyrinato iron (III) (20 mg kg^{-1}). Protein expression was evaluated in MCA and in human microvascular endothelial cells submitted to hypoxia (overnight)/reoxygenation (24 h) (H/R) using immunofluorescence and immunoblotting.

RESULTS: In U46619-preconstricted MCA, EDH-type relaxation by the proteinase-activated receptor 2 agonist serine–leucine–isoleucine–glycine–arginine–leucine–NH_2 (SLIGRL) was greater in I/R than sham rats due to an increased contribution of small-conductance calcium-activated potassium channels (SK_{Ca}), which was confirmed by the enlarged relaxation to the SK_{Ca} activator N-cyclohexyl-N-2-(3,5-dimethyl-pyrazol-1-yl)-6-methyl-4-pyrimidinamine. I/R and H/R induced endothelial protein tyrosine nitration and filamentous-actin disruption. In control MCA, either cytochalasin D or peroxynitrite disrupted endothelial filamentous-actin and augmented EDH-type relaxation. Furthermore, peroxynitrite decomposition during I/R prevented the increase in EDH-type responses.

This article is protected by copyright. All rights reserved.

CONCLUSION: Following TP stimulation in MCA, EDH-type relaxation to SLIGRL is greater after I/R due to endothelial filamentous-actin disruption by peroxynitrite, which prevents TP-induced block of SK_{Ca} input to EDH. These results reveal a novel mechanism whereby peroxynitrite could promote postischemic brain injury.

Keywords: actin; calcium-activated potassium channels; ischemia/reperfusion; $K_{Ca}2.3$; SK_{Ca}; thromboxane

Introduction

The cerebrovasculature is continually exposed to various stimuli (e.g. high arterial pressure, ischemia) that can alter the physiological distribution of cerebral blood flow (CBF). Cerebral arteries possess mechanisms of autoregulation to maintain CBF and protect brain tissue during changes in perfusion pressure (Cipolla 2009). Both nitric oxide (NO) and endothelium-derived hyperpolarization (EDH) are two separate dilator pathways that operate simultaneously to regulate CBF. Several lines of evidence suggest that EDH-mediated responses persist or even increase when NO bioavailability is reduced in different pathological states, including cerebral ischemia-reperfusion (I/R; Marrelli *et al.* 1999, Marrelli 2002, Cipolla *et al.* 2009). Compromised NO signalling is often associated with endothelial cell damage and platelet activation. Thus, EDH-mediated responses may act as a back-up mechanism to maintain endothelium-dependent vasodilation and homeostasis in the brain (Golding *et al.* 2002).

Acute ischemic stroke is a thrombo-inflammatory disorder involving excessive platelet activation (Chamorro 2009). To date, immediate thrombolysis with tissue plasminogen activator is the only pharmacological treatment effective in ischemic stroke (George & Steinberg 2015), but it can develop into progressive damage in a process called “reperfusion

This article is protected by copyright. All rights reserved.

Accepted Article

injury" (Coutts & Goyal 2009). Thromboxane A_2 (TxA_2) is one of the multiple factors released by activated platelets that can mediate further platelet recruitment, activation, and smooth muscle cell constriction, contributing to the prothrombotic state in I/R (Chamorro 2009). In addition, previous studies suggest a role of endothelial thromboxane/prostaglandin receptor (TP) stimulation in suppressing the small-conductance calcium-activated potassium (SK_{Ca}) channel component of EDH (Plane & Garland 1996, Crane & Garland 2004, McNeish & Garland 2007; McNeish *et al.* 2012, Gauthier *et al.* 2014). Thus, TxA_2-induced attenuation of EDH-mediated relaxation may represent an additional mechanism by which TxA_2 could impair tissue perfusion, especially in disease states where NO is defective (Ellinsworth *et al.* 2014).

TxA_2 binds to TP in both smooth muscle and endothelial cells and triggers the RhoA/Rho kinase pathway, which is hyperactivated in the ischemic brain (Koumura *et al.* 2011), regulating many cellular functions including ion channel activity (Ghisdal *et al.* 2003, Luykenaar *et al.* 2009). Rho kinase activation is linked to inhibition of endothelial cell SK_{Ca} channel function in rat middle cerebral artery (MCA; McNeish *et al.* 2012, Gauthier *et al.* 2014), although the precise mechanism is still unknown. One possibility is that inhibition of SK_{Ca} channel function is dependent upon actin cytoskeleton remodelling (Gorovoy *et al.* 2005, Prasain & Stevens 2009). Therefore, we hypothesize that modulation of endothelial cell actin cytoskeleton is necessary for TP-dependent inhibition of SK_{Ca} channel function and EDH-type relaxation. Interestingly, I/R is associated with increased peroxynitrite formation and disruption of cerebral smooth muscle actin (Maneen *et al.* 2006, Maneen & Cipolla 2007, Coucha *et al.* 2013). Therefore, we also explored whether peroxynitrite alters the endothelial actin cytoskeleton, and interferes with TP-dependent inhibition of SK_{Ca} channel function. Our results suggest that increased peroxynitrite production during I/R leads to endothelial cell F-actin disruption, which prevents TP-induced block of SK_{Ca} channel input to EDH, increasing proteinase-activated receptor (PAR) 2-evoked EDH-type relaxation. These findings reveal a novel mechanism whereby EDH may compensate loss of NO-mediated

This article is protected by copyright. All rights reserved.

Accepted Article

relaxation in prothrombotic disease states such as ischaemic stroke. We propose that these alterations, however, could have potential deleterious effects on the injured brain.

Materials and Methods

Animals

The animal studies are reported as recommended by the ARRIVE guidelines (Kilkenny *et al.* 2010) and the study is conforming with: Good publication practice in physiology. Acta Physiol (Oxf). 2015 Dec;215(4):163-4. One hundred and thirty-five adult male Sprague-Dawley rats (Harlan; 270 to 330 g body weight) were used. Rats were housed under a 12:12-h light-dark cycle, controlled environmental conditions of temperature and humidity, and provided with access to food and water ad libitum. All of the experiments were carried out under the Guidelines established by the Spanish legislation (RD 1201/2005) and according to the guidelines for the European Community Council Directive (2010/63/EU) for Protection of Vertebrate Animals Used for Experimental and other Scientific Purposes. Experiments were approved by the Ethics Committee of the Universitat Autònoma de Barcelona.

Transient middle cerebral artery occlusion model

Rats were anesthetized with isoflurane (3.5%) in a mixture of O_2 and N_2O (30:70). Focal brain ischemia was produced by 90-min intraluminal occlusion of the right MCA with reperfusion (24 h) as reported previously (Pérez-Asensio *et al.* 2010, Onetti *et al.* 2015). Sham-operated (sham) rats were subjected to all the surgical procedures and the filament was introduced in the MCA and immediately removed. Cortical CBF, assessed with a laser–Doppler system (Perimed AB, Järfalla, Sweden), was monitored, and body temperature was maintained at 37 ± 0.5 °C during surgery. To produce analgesia, buprenorphine (0.01 mg kg^{-}

This article is protected by copyright. All rights reserved.

Accepted Article

[1]) was administered subcutaneously 15 min before recovery from the anaesthesia. At 24 h after MCA occlusion, they were deeply anesthetized with isoflurane (5%) and decapitated. The presence of an infarcted area, assessed by 2,3,5-triphenyltetrazolium chloride (Sigma-Aldrich, St. Louis, MO, USA) staining, was the criteria to determine that I/R was successful (Pérez-Asensio *et al.* 2010, Onetti *et al.* 2015). In some experiments, non-operated rats of the same sex and body weight that were not subjected to surgery were used as controls.

In a set of animals, rats were treated (i.p.) 10 min after the onset of ischemia with either the peroxynitrite decomposition catalyst 5,10,15,20-tetrakis(4-sulfonatophenyl)prophyrinato iron (III) (FeTPPS; 20 mg kg^{-1}; Calbiochem, San Diego, CA, USA; Kunz *et al.* 2007, Coucha *et al.* 2013) or vehicle (saline). The dose used was previously shown to inhibit the peroxynitrite-induced F-actin protein tyrosine nitration-effects on MCA myogenic function after I/R (Coucha *et al.* 2013).

Middle cerebral artery preparation

Brain was removed and placed in ice-cold Krebs-Henseleit solution (KHS - in mmol L^{-1}: 112.0 NaCl, 4.7 KCl, 2.5 $CaCl_2$, 1.1 KH_2PO_4, 1.2 $MgSO_4$, 25.0 $NaHCO_3$, and 11.1 glucose) continuously gassed with 95% O_2 and 5% CO_2. Segments of MCA (wire and pressure myography and immunofluorescence studies) were dissected and maintained in cold KHS. For immunofluorescence studies, arteries were fixed with 4% phosphate-buffered paraformaldehyde (PFA; pH 7.4) for 1 h and washed in three changes of phosphate buffered-saline solution (PBS; pH 7.4). After clearing, arterial segments were placed in PBS containing 30% sucrose overnight, transferred to a cryomold (Bayer Química Farmacéutica, Barcelona, Spain) containing Tissue Tek OCT embedding medium (Sakura Finetek Europe, Zoeterwoude, The Netherlands), frozen in liquid nitrogen, and kept at −70 °C.

This article is protected by copyright. All rights reserved.

Accepted Article

Wire myography

MCA function was studied in vessels mounted on an isometric wire myograph (model 410 A; Danish Myo Technology, Aarhus, Denmark) following the protocol described (McNeish *et al.* 2012, Gauthier *et al.* 2014). Constricted tone was induced with the stable TxA_2 mimetic 9,11-Dideoxy-9α,11α-methano-epoxy prostaglandin F2α (U46619; 30-100 nmol L^{-1}; EMD Millipore, Billerica, MA, USA) or endothelin-1 (1-10 nmol L^{-1}; Enzo Life Sciences Inc., Farmingdale, NY, USA). Contractions were maintained around 60-80% of tone obtained with KCl (100 mmol L^{-1}), before adding the relaxing agonists. Endothelial-dependent relaxations were obtained with the agonist of proteinase-activated receptor (PAR) 2 serine–leucine–isoleucine–glycine–arginine–leucine–NH2 (SLIGRL; 20 μmol L^{-1}; Auspep, Tullamarine, Victoria, Australia), bradykinin (1 nmol L^{-1}-30 mmol L^{-1}; Sigma-Aldrich, St. Louis, MO, USA), or the potent and selective activator of small-conductance calcium-activated potassium (SK_{Ca}) channels N-cyclohexyl-N-2-(3,5-dimethyl-pyrazol-1-yl)-6-methyl-4-pyrimidinamine (CyPPA; 100 μmol L^{-1}; Sigma-Aldrich, St. Louis, MO, USA; Hougaard *et al.* 2007). A single concentration of SLIGRL was used to minimize potential desensitization of PAR2 (Hwa *et al.* 1996, Bucci *et al.* 2005). Preliminary experiments showed that it was not possible to obtain reliable cumulative concentration-dependent MCA relaxations to CyPPA.

The effects of the non-selective nitric oxide synthase inhibitor Nω-nitro-l-arginine methyl ester (l-NAME; 300 μmol L^{-1}; Sigma-Aldrich, St. Louis, MO, USA), the nonselective cyclooxygenase (COX) inhibitor indomethacin (10 μmol L^{-1}; Sigma-Aldrich, St. Louis, MO, USA), the specific intermediate-conductance K_{Ca} (IK_{Ca}) channel blocker TRAM-34 (1 μmol L^{-1}; Sigma-Aldrich, St. Louis, MO, USA), the specific SK_{Ca} channel blocker apamin (100 nmol L^{-1}; Latoxan, Valence, France), or the IK_{Ca} and large-conductance K_{Ca} (BK_{Ca}) channel blocker charybdotoxin (100 nmol L^{-1}; Latoxan, Valence, France) on endothelium-dependent relaxation were investigated by their addition 30 min before vessel preconstriction. Concentrations of most inhibitors were chosen based on previous studies (McNeish & Garland 2007, McNeish *et al.* 2012, Gauthier *et al.* 2014). Preliminary experiments were

This article is protected by copyright. All rights reserved.

conducted to obtain the adequate concentration of the actin cytoskeleton disruptor cytochalasin D (50 nmol L^{-1}; EMD Millipore, Billerica, MA, USA) that did not affect vessel preconstriction, and either cytochalasin D or another actin cytoskeleton disruptor latrunculin B (10 nmol L^{-1}-1 μmol L^{-1}; EMD Millipore, Billerica, MA, USA) were added 30 min before starting the experiment.

The potent oxidizing and nitrating agent peroxynitrite (EMD Millipore, Billerica, MA, USA) was added 30 min before vessel preconstriction at a concentration of 5 μmol L^{-1} to affect vascular K_{Ca} channel activity (Liu *et al.* 2002). Preliminary experiments were conducted to obtain the adequate concentration of the oxidation/nitration inhibitor epicatechin (1 μmol L^{-1}; Sigma-Aldrich, St. Louis, MO, USA) and the cytoskeleton stabilizer jasplakinolide (100 nmol L^{-1}; EMD Millipore, Billerica, MA, USA) that did not affect vessel preconstriction, and were added 10 min before addition of peroxynitrite and maintained during peroxynitrite incubation. Decomposed-peroxynitrite (5 μmol L^{-1}) was also used and added 30 min before vessel preconstriction. The activity of peroxynitrite and its decay after decomposition was confirmed by spectrophotometry according to the method described by Balavoine & Geletti (1999). Briefly, consumption of pyrogallol red (6 μmol L^{-1}; Sigma-Aldrich, St. Louis, MO, USA) by peroxynitrite (2 μmol L^{-1}), submitted or not to different conditions (no degradation, 4 h of light exposure, overnight incubation at 37 °C, overnight incubation at room temperature), was evaluated in the presence of diphenyl diselenide (Sigma-Aldrich, St. Louis, MO, USA), and absorbance was measured at 540 nm.

Middle cerebral artery endothelial filamentous-actin staining

The ipsilateral MCA from sham, I/R or non-operated (control) rats was mounted in a small vessel pressure myograph (model P100; Danish Myo Technology, Aarhus, Denmark) following the protocol previously described (Onetti *et al.* 2015). Arteries from control rats were incubated (30 min) with cytochalasin D (50 nmol L^{-1}) or peroxynitrite (5 μmol L^{-1}). All

This article is protected by copyright. All rights reserved.

Accepted Article

arteries were set to 70 mmHg in 0 Ca^{2+}-KHS, pressure-fixed with 4% PFA in 0.2 mol L^{-1} phosphate buffer (pH 7.2-7.4) for 45 min, and stored overnight in PFA (4%) at 4 °C. Pressured-fixed intact arteries were mounted on slides in a well that was made of silicon spacers (to avoid artery deformation) and were double stained with the filamentous (F)-actin dye Alexa Fluor® 568 Phalloidin (Thermo Fisher Scientific Inc., Kalamazoo, MI, USA), following the manufacturer's instructions, and the nuclear dye Hoechst 33342 (0.01 mg mL^{-1}; Sigma-Aldrich, St. Louis, MO, USA). Arteries were imaged with a Leica TCS SP5 (Manheim, Germany) confocal system at x63, at 561-nm (F-actin) and 405-nm (nuclei). Two or more stacks of serial optical slices (0.4-µm thick), from different regions containing at least two endothelial cell nuclei, were captured in each arterial segment, starting at the first emerging endothelial cell and proceeding into the lumen of each artery. Every image was taken under identical conditions of zoom (x4.5), laser intensity, brightness, and contrast. 3D image analysis was performed with Imaris 8.1 Image Analysis software (Bitplane, Oxford Instruments, Abingdon, UK). We defined two cuboid regions of interest (ROI) per stack, coinciding with the nuclear and cytoplasmic region of an endothelial cell, which remained constant for each artery. The average fluorescence intensity and volume of F-actin objects within each ROI was measured in the Z-axis (8-µm stack depth).

Microvascular endothelial cell culture and hypoxia/reoxygenation model

Human microvascular endothelial cell (HMVEC) lines from two different batches were obtained from Thermo Fisher Scientific Inc. (Kalamazoo, MI, USA), maintained in culture in phenol red-free DMEM-F12 supplemented with 10% (v/v) foetal bovine serum (FBS) and microvascular growth supplement (Thermo Fisher Scientific Inc., Kalamazoo, MI, USA), and incubated at 37 °C in a humidified atmosphere at 95% air and 5% CO_2. Cells were plated onto 1% gelatine-coated culture dishes and studied before confluence between passages 5 and 7. To induce hypoxia/reoxygenation (H/R), culture medium was changed to charcoal-

This article is protected by copyright. All rights reserved.

Accepted Article

striped low-serum (1%) media and cells were placed inside a sealed chamber. Hypoxic conditions were created by injection in the chamber with 94% N_2, 5% CO_2 and 1% O_2 and hypoxia incubation proceeded overnight. In normoxic conditions, cells were kept overnight in the humidified atmosphere incubator with charcoal-striped low-serum (1%) media. Following hypoxia, cells were washed with PBS, fresh supplemented with DMEM-F12 + 10% FBS and reoxygenated in the humidified atmosphere incubator to simulate reperfusion conditions (Koo *et al.* 2001). After 24 h of reoxygenation, HMVEC were treated with U46619 (100 nmol L^{-1}) for 15 min. In a series of experiments, normoxic cells were treated with peroxynitrite (500 nmol L^{-1}) for 2 h and processed accordingly to each experimental protocol. It was not possible to use the same concentration of peroxynitrite used in experiments of vascular function (5 µmol L^{-1}), since this concentration considerably affected cell viability.

Immunofluorescence

The ipsilateral MCA from sham, I/R or control rats was used. Arteries from control rats were incubated with peroxynitrite (5 µmol L^{-1}; 30 min; in KHS at 37 °C) before being processed for immunofluorescence studies. Frozen transverse sections (14-µm thick) of MCA were incubated (1 h) with a rabbit polyclonal antibody against SK_{Ca} channels (1:100; Alomone labs, Jerusalem, Israel) or nitrotyrosine (1:100; Millipore, Billerica, MA, USA). After washing, sections were incubated (45 min) with the secondary antibody (1:200), a donkey anti-rabbit IgG conjugated to Cyanine 3 (Jackson ImmunoResearch Laboratories Inc., West Grove, PA, USA) at 37 °C. Sections were processed for immunofluorescence staining essentially as described (Onetti *et al.* 2015). The specificity of the immunostaining was verified by omission of the primary antibody and processed as above, which abolished the fluorescence signal.

HMVEC grown on coverslips were washed with ice-cold PBS and fixed with 4% PFA. After permeabilization with 0.1% Triton X-100/0.1% bovine serum albumin in PBS for 5 min and blockage with 10% horse serum in PBS for 15 min, cells were incubated in blocking solution

This article is protected by copyright. All rights reserved.

Accepted Article

for 1 h at room temperature with primary antibodies: SK_{Ca} channels (1:100; Alomone labs, Jerusalem, Israel) or nitrotyrosine (1:100; Millipore, Billerica, MA, USA). Following washes, cells were co-stained with fluorescence-conjugated phalloidin (10 μM; Sigma-Aldrich, St. Louis, MO, USA) for F-actin and deoxyribonuclease I (300 nM; Thermo Fisher Scientific Inc., Kalamazoo, MI, USA) for globular (G)-actin, and secondary antibodies (1:500) Alexa Fluor 594 conjugated goat anti-rabbit for SK_{Ca} channels and Alexa Fluor 488 conjugated goat anti-rabbit (Thermo Fisher Scientific Inc., Kalamazoo, MI, USA) for nitrotyrosine. Coverslips were mounted on slides using ProLong Gold antifade reagent with DAPI (Thermo Fisher Scientific Inc., Kalamazoo, MI, USA), and visualized through a confocal microscope (Axiovert 2000, Carl Zeiss Iberia, S.L., Spain) with a x63 objective lens (Carl Zeiss Iberia, S.L., Spain). Images were taken from 15-20 cells per coverslip.

Western blotting

Equal amount of protein from each cell sample (25 μg) was resolved by SDS-PAGE on 4-12% gels and electroblotted onto nitrocellulose. Membranes were incubated overnight at 4 °C in PBS with 0.1% (v/v) Tween 20 (PBST) containing 2% milk and specified polyclonal rabbit primary antibodies (1:500) as follows: anti-SK_{Ca} channels (Alomone labs, Jerusalem, Israel); anti-nitrotyrosine (Millipore, Billerica, MA, USA); or anti HIF-1α (Millipore, Billerica, MA, USA). After incubation with horseradish peroxidase-labelled specific secondary antibodies in PBST containing 1% milk and additional washes, chemiluminescent signal was visualized by LAS4000 imaging system (Fujifilm, Barcelona, Spain). Densitometric analyses of Western blots were performed using a Mac Biophotonic ImageJ Software. All membranes were reblotted using a monoclonal antibody anti GAPDH (1:2500; Santa Cruz Biotechnology, Santa Cruz, CA, USA) as a loading control. Data were normalized to corresponding values of GAPDH densitometry.

This article is protected by copyright. All rights reserved.

Accepted Article

Accepted Article

Endothelial cell filamentous/globular-actin measurements

Cells were grown on 60 mm dishes and went through H/R and treatment processes as described above. Subsequently, cells were washed once in ice-cold PBS before lysis with actin stabilization buffer (Cytoskeleton, Denver, CO, USA) on ice for 10 min. Cells were dislodged by scraping and the entire extract was incubated at 37 °C for 10 min. Samples were ultra-centrifuged (100,000 g) for 1 h at 37 °C. The supernatant containing globular (G)-actin was recovered, and the pellet containing F-actin was solubilized with actin depolymerisation buffer (Cytoskeleton, Denver, CO, USA). Aliquots of supernatant and pellet fractions were separated on 4-12% SDS-PAGE gels and then immunoblotted with monoclonal anti-actin antibody (Cytoskeleton, Denver, CO, USA). Chemiluminescent signal was detected by chemiluminescent reagent according to the manufacturer's protocols (SuperSignal west pico, Thermo Fisher Scientific Inc., Kalamazoo, MI, USA), and visualized by LAS4000 imaging system (Fujifilm, Barcelona, Spain).

RhoA activation pull-down assay

Cells were grown on 60 mm dishes. After H/R and treatment processes described above, cells were cross-linked with Coupling Buffer (0.01 mol L^{-1} sodium phosphate, 0.15 mol L^{-1} NaCl; 20 µg mL^{-1} disuccinimidyl suberate; pH 7.2). Cells were washed twice in PBS, incubated for 10 min in Mg^{++} lysis buffer (MLB; 25 mmol L^{-1} HEPES, pH 7.5, 150 mmol L^{-1} NaCl, 1% Igepal CA-630, 10 mmol L^{-1} $MgCl_2$, 1 mmol L^{-1} EDTA and 2% glycerol). Cell lysates were harvested by scraping and nuclei were collected by centrifugation (5 min, 14,000 g, 4 °C). Equal amount of protein (50 µg) was incubated overnight at 4 °C with Rhotekin RBD agarose (Millipore, Billerica, MA, USA) containing 65 µg of recombinant Rho binding domain protein in 50 µL of glutathione-agarose slurry. After 3 washes with MLB and proper elution by boiling in Laemmli reducing buffer, samples were separated on 4-12% SDS-PAGE gels and then immunoblotted with monoclonal anti-RhoA antibody (1:1000;

This article is protected by copyright. All rights reserved.

Santa Cruz Biotechnologies, Santa Cruz, CA, USA). Cell extracts from a serum-starved state (low basal RhoA activity) were used as negative control. Positive controls were aliquots treated with 100 μmol L^{-1} of GTPγS non-hydrolyzable analog to activate RhoA. Pull-down signal was normalized by total RhoA signal in aliquots of cell lysates not loaded with Rhotekin RBD agarose.

Statistical analysis

Results are expressed as mean ± SEM of the number (*n*) of arteries from different animals or independent cell culture experiments indicated in the figure legends. Vasodilator responses were expressed as the percentage change of the previous tone calculated by subtracting resting tone from U46619 or endothelin-1 contraction. A two-way ANOVA followed by Tukey's post-test was used, when appropriate. In the case of one single factor, unpaired Student's *t*-test or one-way ANOVA followed by Tukey's post-test was used for two or more than two groups, respectively. Data analysis was carried out using GraphPad Prism version 4 software. A value of $P < 0.05$ was considered significant.

Results

Influence of U46619 stimulation on EDH-type MCA relaxation after I/R

Endothelium-dependent relaxation to SLIGRL (20 μmol L^{-1}) following preconstriction with U46619 (30-100 nmol L^{-1}) was impaired in MCA from the ischemic ipsilateral (103.50 ± 3.64%; $n = 15$) compared to the non-ischemic contralateral hemisphere (124.62 ± 4.64%; $P < 0.05$; $n = 12$) or sham (128.76 ± 4.45%; $P < 0.01$; $n = 24$) vessels. However, when arteries were treated with l-NAME (300 μmol L^{-1}) plus indomethacin (10 μmol L^{-1}), SLIGRL evoked larger EDH-type relaxation in U46619-preconstricted ipsilateral ($P < 0.01$), but not

This article is protected by copyright. All rights reserved.

Accepted Article

contralateral, MCA compared to sham (Fig. 1a). All further experiments of arterial function involving I/R animals were performed in ipsilateral MCA. Bradykinin evoked concentration-dependent EDH-type relaxation in vessels preconstricted with U46619 that was similar between I/R and sham arteries (Figure S1). When MCA were preconstricted with endothelin-1 (1-10 nmol L^{-1}), relaxations to SLIGRL were equally small in MCA from I/R (22.54 ± 9.55%; n = 5) and sham (34.29 ± 7.33%; n = 4) rats.

Effect of K_{Ca} channel blockers on EDH-type MCA relaxation after I/R

The specific IK_{Ca} channel blocker TRAM-34 (1 μmol L^{-1}) reduced SLIGRL relaxation in U46619-preconstricted MCA from both I/R and sham animals (Fig. 1b, c). However, the degree of EDH-type relaxation was still greater (P < 0.05) in I/R than sham arteries. The specific SK_{Ca} channel blocker apamin (100 nmol L^{-1}) diminished (P < 0.001) EDH-type relaxations in I/R, but not sham arteries. Addition of TRAM-34 plus apamin similarly reduced EDH-type relaxation in I/R and sham arteries. Comparing incubation of TRAM-34 alone with TRAM-34 plus apamin, EDH-type relaxation only decreased (P < 0.01) in the I/R group (Fig. 1b, c). In all groups, EDH-type responses were abolished in the presence of a combination of apamin with the IK_{Ca} and BK_{Ca} channel blocker charybdotoxin (100 nmol L^{-1}; results not shown).

Rho-mediated signal activation in HMVEC submitted to H/R

Although H/R in isolated cells does not recapitulate all aspects of I/R injury, it provides an interesting model for studying the molecular mechanisms involved in the increased EDH-type relaxation in MCA after I/R. We submitted HMVEC to H/R, a cell culture model of I/R (Koo *et al.* 2001). As observed in Figure 2a and S2, expression of hypoxia-inducible factor 1α (HIF-1α) was higher in cells that have undergone H/R than in those kept in normoxia.

This article is protected by copyright. All rights reserved.

Accepted Article

Accepted Article

These results suggest that our cell system is a suitable model for H/R in endothelial cells. Rho activation is an important regulator of the activity of some ion channels (Ghisdal *et al.* 2003, Luykenaar *et al.* 2009), which may play a role on TP-dependent inhibition of SK_{Ca} channel function in the endothelium (McNeish *et al.* 2012, Gauthier *et al.* 2014). We analysed GTP-bound RhoA levels as a measure of RhoA activation (Fig. 2b), and found that 15-min treatment with U46619 increased RhoA activity in both control ($P < 0.05$) and H/R ($P < 0.001$) conditions. It is important to note that H/R *per se* did not modify RhoA activity, but markedly augmented ($P < 0.01$) RhoA activation following U46619 stimulation. These results suggest an exaggerated TP-mediated RhoA activation after H/R in comparison to control conditions.

SK_{Ca} channel expression

To determine if I/R-induced increase in SK_{Ca} channel signalling is related to changes in SK_{Ca} channel levels, we measured SK_{Ca} channel protein expression in both HMVEC and rat MCA (Fig. 3). We observed that neither U46619 stimulation nor exposure to H/R altered SK_{Ca} channel protein levels in HMVEC, as assessed by Western blotting (Fig. 3a and S3). We also studied protein levels, assessed by immunofluorescence, of SK_{Ca} channels in HMVEC (Fig. 3b) and MCA cross sections from sham and I/R rats (Fig. 3c). SK_{Ca} channel fluorescence was similar in control and H/R HMVEC (Fig. 3b). Positive red immunofluorescence signal for SK_{Ca} channels was restricted to the adventitia and endothelial layers of the MCA, and was similar in sham and I/R arteries (Fig. 3c).

This article is protected by copyright. All rights reserved.

Accepted Article

Actin content and distribution

The content and distribution of F- and G-actin in HMVEC is shown in Figure 4. Exposure of endothelial cells to H/R led to a decrease in F-actin fluorescence (Fig. 4a) that was paralleled by a marked decrease ($P < 0.001$) in the amount of F-actin (Fig. 4b), while G-actin expression remained unaffected (Fig. 4a, b). No appreciable differences on F- and G-actin were observed after U46619 incubation when compared to its own control (Fig. 4a, b). Similar to H/R, exogenous peroxynitrite (500 nmol L^{-1}) was able to reduce both the F-actin fluorescence (Fig. 4a) and the F/G actin ratio (Fig. 4b) in HMVEC. In intact and pressurized MCA, endothelial F-actin object volume, but not fluorescence, was decreased ($P < 0.05$) in I/R versus sham arteries (Fig. 4c). Similarly, incubation of MCA from non-operated (control) rats with cytochalasin D (50 nmol L^{-1}) or peroxynitrite (5 µmol L^{-1}) was without effect on F-actin fluorescence, but significantly diminished ($P < 0.05$) F-actin object volume (Fig. 4c).

Effect of actin cytoskeleton disruption on EDH-type relaxation of control MCA

The role of actin organization on EDH-type vasodilation following TP stimulation was evaluated by using different agents that disrupt actin cytoskeleton at doses that did not affect U46619-preconstriction. We first studied the effect of different concentrations of the actin filament assembly inhibitor latrunculin B (Spector *et al.* 1989) on EDH-type responses in MCA from non-operated (control) rats, as these arteries showed a similar EDH-type response following TP stimulation than sham arteries (Fig. 5). Latrunculin B did not modify the basal tone (Table S1), and induced a progressive decrease of EDH-type relaxation in control arteries (Fig. 5a). We next tested the effect of cytochalasin D, an actin cytoskeleton-disrupting agent that acts by a different mechanism than latrunculin B. Cytochalasin D induces barbed end capping and, at higher doses, severing of actin filaments, which progressively depolymerize actin polymers (Wakatsuki *et al.* 2001). In contrast to latrunculin B, exposure of control arteries to cytochalasin D (50 nmol L^{-1}) did potentiate ($P < 0.01$) EDH-

This article is protected by copyright. All rights reserved.

type relaxation (Fig. 5b), without altering the basal tone (Table S1). The cytochalasin D-induced potentiation of the EDH-type response was significantly diminished by incubation of apamin and TRAM-34, alone or in combination (Fig. 5b). To confirm the presence of SK_{Ca} channel input to EDH, we selectively activated SK_{Ca} channels with CyPPA (100 μmol L^{-1}; Hougaard *et al.* 2007), which induced a higher (P < 0.01) relaxation in cytochalasin D-incubated than control arteries (Fig. 5c). Lastly, addition of apamin significantly reduced (P < 0.001) CyPPA relaxation in cytochalasin D, but not in control (P = 0.220), arteries.

Detection of protein tyrosine nitration

Immunofluorescent and Western blot analysis of protein tyrosine nitration showed an increase (P < 0.001) in nitrotyrosine fluorescence/expression in HMVEC exposed to H/R (Fig. 6a, b and S4), comparable to levels seen when cells were treated with peroxynitrite (500 nmol L^{-1}; Fig. 6b). In MCA cross sections, a weak nitrotyrosine fluorescent signal was found in sham arteries, whereas after I/R, marked protein tyrosine nitration was observed in all three layers of the vessel wall, including the endothelial layer (Fig. 6c). Similar to I/R, exogenous incubation of control MCA with peroxynitrite (5 μmol L^{-1}) also promoted marked protein tyrosine nitration of the vessel wall, including the endothelial layer.

Impact of exogenous peroxynitrite on EDH-type relaxation of control MCA

Subsequent experiments examined the effect of peroxynitrite (5 μmol L^{-1}) exposure on EDH-type relaxation after U46619 preconstriction in arteries from control rats (Fig. 7a, b). Incubation of MCA with peroxynitrite did not modify the basal tone (Table S1), but increased (P < 0.01) the SLIGRL-evoked EDH-type relaxation (Fig. 7a). Inhibition of protein oxidation/nitration with epicatechin (1 μmol L^{-1}) or induction of F-actin stabilization with jasplakinolide (100 nmol L^{-1}) was not associated with increased EDH-type relaxation by

This article is protected by copyright. All rights reserved.

Accepted Article

peroxynitrite. In addition, exposure of control arteries to decomposed-peroxynitrite (5 μmol L^{-1}), obtained by submitting peroxynitrite to overnight incubation at 37 °C (Figure S5), was unable to potentiate EDH-type responses (Fig. 7a). Peroxynitrite-induced potentiation of the EDH-type response was significantly diminished by incubation of apamin and TRAM-34, alone or in combination (Fig. 7b). In addition, EDH-type relaxation decreased ($P < 0.05$) when comparing incubation of TRAM-34 alone with TRAM-34 plus apamin. Furthermore, CyPPA relaxation augmented ($P < 0.01$) after peroxynitrite, but not decomposed-peroxynitrite, exposure (Fig. 7c).

Effect of catalytically decomposing endogenous peroxynitrite on EDH-type MCA relaxation after I/R

To determine the *in vivo* effect of peroxynitrite formed during I/R on EDH-type relaxation following TP stimulation in MCA, rats were treated with FeTPPS (20 mg kg^{-1}), a selective peroxynitrite decomposition catalyst (Kunz *et al.* 2007, Coucha *et al.* 2013), or saline (vehicle; Fig. 7d, e). Body weight, body temperature and percentage changes in cortical CBF during surgery are shown in Table S2. I/R rats treated with vehicle showed a larger ($P < 0.01$) EDH-type relaxation than vehicle-treated sham or FeTPPS-treated I/R rats (Fig. 7d). Addition of TRAM-34 alone or TRAM-34 plus apamin reduced EDH-type relaxation in any group compared to non-treated arteries. Remarkably, comparing incubation of TRAM-34 alone with TRAM-34 plus apamin, EDH-type relaxation only significantly decreased ($P < 0.001$) in I/R rats treated with vehicle, suggesting the presence of SK_{Ca} channel input to EDH (Fig. 7d). Consistent with this, CyPPA-mediated relaxation was larger ($P < 0.01$) in MCA from vehicle-treated I/R than sham rats, and this effect was prevented by apamin incubation or *in vivo* FeTPPS treatment (Fig. 7e).

This article is protected by copyright. All rights reserved.

Accepted Article

Accepted Article

Discussion

Results from the present study show that PAR2-evoked EDH-type relaxation is greater in U46619-preconstricted MCA of I/R compared to sham rats. We demonstrate that the increased EDH-type relaxation of the MCA after I/R is due to the inability of TP stimulation to block the SK_{Ca} channel EDH. We propose that the underlying mechanism involves increased peroxynitrite production and endothelial cell F-actin disruption during I/R.

An increase in EDH-type MCA relaxation of the basal tone to uridine 5'-triphosphate has been reported after cerebral I/R (Marrelli *et al.* 1999, Marrelli 2002). In the present study, I/R only potentiated EDH-type responses to SLIGRL in U46619-preconstricted arteries, suggesting the involvement of specific receptor activation. Similarly, PAR2 signalling is unaltered with stroke in the MCA of stroke-prone spontaneously hypertensive rats (Smeda & McGuire 2007). Previous evidence suggests that increases in EDH-type MCA relaxation after cerebral I/R could be triggered by a mechanism involving K_{Ca} channels (Marrelli *et al.* 1999). These observations were followed by studies demonstrating that K_{Ca} channels mediate the EDH response in rat MCA (McNeish *et al.* 2005, McNeish *et al.* 2006). Thus, it is plausible that augmented EDH-type relaxation following I/R is achieved through an increase of K_{Ca} channel signalling. We demonstrate SK_{Ca} channels are expressed in the endothelial layer of rat MCA, consistent with previous observations (McNeish *et al.* 2006), and that SK_{Ca} channels are also detected within the adventitia. Interestingly, SK_{Ca} channel expression was unaltered after I/R, as reported in parenchymal arterioles branching from the MCA (Cipolla *et al.* 2009).

When the MCA is able to synthesize NO, both IK_{Ca} and SK_{Ca} channels contribute to EDH responses. However, under NO-deprived (McNeish *et al.* 2006) or TP-stimulated (McNeish & Garland 2007) conditions, the SK_{Ca} channel component of EDH is blocked. SK_{Ca} channel activity can be restored by exposure to COX inhibitors or TP antagonists (McNeish & Garland 2007; McNeish *et al.* 2012, Gauthier *et al.* 2014), demonstrating a role for TP

This article is protected by copyright. All rights reserved.

stimulation in suppressing SK_{Ca} channel function (Plane & Garland 1996, Crane & Garland 2004, McNeish & Garland 2007). Indeed, U46619-preconstricted MCA from sham rats had no SK_{Ca} channel component to EDH-type relaxation. Surprisingly, we found that the SK_{Ca} channel input to EDH-type responses was restored after I/R, increasing EDH-type relaxation compared to sham arteries. Whilst following I/R there was still an IK_{Ca} channel component to EDH-type relaxation, SK_{Ca} appeared to be the dominant channel as apamin virtually abolished relaxation and the residual relaxations were not inhibited to a greater extent by additional blockade of IK_{Ca} channels. In addition, direct stimulation of SK_{Ca} channels with the selective SK_{Ca} channel activator CyPPA (Hougaard *et al.* 2007) induced a greater relaxation in I/R than sham arteries. Together, these findings suggest that I/R has direct effects on SK_{Ca} channel activity independent of other components of the EDH response, and thus we focussed on the effect of I/R on this channel throughout the rest of the study.

Activity of ion channels in numerous tissues is regulated by the actin cytoskeleton and cytoskeletal elements are responsible for localization and clustering of channel molecules in the plasma membrane (Levina *et al.* 1994). We found that H/R causes disruption of actin filaments in isolated endothelial cells. In parallel, cytochalasin D-induced depolymerisation of actin polymers (Spector *et al.* 1989, Wakatsuki *et al.* 2001), but not latrunculin B-induced prevention of actin monomer polymerization (Spector *et al.* 1989), augments the SK_{Ca} channel input to EDH-type relaxation in the MCA. Furthermore, cytochalasin D also increased direct SK_{Ca} channel relaxation evoked by CyPPA. Together, these results suggest the presence of an intact endothelial cell actin cytoskeletal preformed network is essential to TP-dependent inhibition of SK_{Ca} channel-mediated relaxation. Similarly, an intact actin cytoskeleton is necessary for Rho kinase inhibition of smooth muscle cell delayed-rectifier potassium channel activity, thus facilitating cerebral artery depolarization and constriction (Luykenaar *et al*. 2009). As TP-dependent inhibition of SK_{Ca} channel function has also been associated with Rho kinase activation in rat MCA (McNeish *et al.* 2012), we investigated if such regulation could be related to the effect of Rho kinase on reorganization of the

This article is protected by copyright. All rights reserved.

Accepted Article

endothelial cell actin cytoskeleton (Gorovoy *et al.* 2005, Luykenaar *et al.* 2009, Prasain & Stevens 2009). We found greater activation of Rho kinase after U46619 stimuli in endothelial cells that underwent H/R than those under normoxic conditions, although it was not able to restore the actin disruption observed. Clearly, more detailed examination is required to determine the mechanism by which endothelial cell actin cytoskeleton influences SK_{Ca} channel activity. However, correct SK_{Ca} channel anchoring to cytoskeleton-binding proteins is essential for channel trafficking and activity (Lu *et al.* 2009, Rafizadeh *et al.* 2014).

I/R is often associated with increased generation of reactive oxygen and nitrogen species, which react rapidly to form peroxynitrite (Yasmin *et al.* 1997). Peroxynitrite is known to contribute to the brain ischemic tolerance and protection afforded by lipopolysaccharide preconditioning (Kunz *et al.* 2007). In addition, peroxynitrite directly affects BK_{Ca} activity (Brzezinska *et al.* 2000, Liu *et al.* 2002, Li *et al.* 2005) and alters function of other proteins by causing both oxidation and posttranslational nitration of tyrosine residues (Palomares & Cipolla 2011). Actin is a tyrosine-rich protein and cerebral artery smooth muscle F-actin nitration is observed in conditions of increased peroxynitrite production, such as I/R, leading to myogenic tone impairment in cerebral arteries (Maneen *et al.* 2006, Maneen & Cipolla 2007, Coucha *et al.* 2013). In the present study, we observed increased protein tyrosine nitration and decreased F/G-actin ratio in HMVEC exposed to peroxynitrite that was similar to cells submitted to H/R. Furthermore, in rat MCA, endothelial protein tyrosine nitration was coupled to F-actin fragmentation either after I/R or peroxynitrite exposure. Incubation of control arteries with peroxynitrite also prevented the U46619-induced block of SK_{Ca} component of EDH-type relaxation and even potentiated these responses, which were similar to those observed after I/R. It is unlikely that other substances derived from the peroxynitrite molecule could be responsible for these effects, as decomposed peroxynitrite did not modify EDH-type relaxation. We then assessed if peroxynitrite generated during I/R was involved in augmenting MCA SK_{Ca}-mediated relaxation. Rats were treated with FeTPPS, a selective peroxynitrite decomposition catalyst (Coucha *et al.* 2013, Kunz *et al.*

This article is protected by copyright. All rights reserved.

Accepted Article

2007), early after occlusion onset to avoid peroxynitrite effects before treatment. The MCA from rats submitted to I/R and treated with FeTPPS showed the U46619-induced block of SK_{Ca} channel relaxation, resulting in similar EDH-type responses to the sham-vehicle group. Together, these findings suggest that peroxynitrite formed during I/R helps prevent loss of EDH-type relaxation following TP stimulation in the MCA, through a mechanism that involves the preservation of SK_{Ca} channel activity.

It is not clear at this stage if peroxynitrite-induced disruption of endothelial F-actin is the only contributor to augmented EDH-type responses. Indeed, other oxidative stress-derived molecules produced during I/R such as superoxide anion and hydrogen peroxide may potentially disrupt the actin cytoskeleton (Moldovan *et al.* 1999, Dalle-Donne *et al.* 2001, Boardman *et al.* 2004). Besides, several studies suggest that oxidative stress can potentiate Ca^{2+} release from endothelial stores (Edwards *et al.* 2008, Lock *et al.* 2012) and enhance endothelial K_{Ca} channel-induced relaxation (Edwards *et al.* 2008). Interestingly, I/R is associated with augmented endothelial Ca^{2+} responses in the rat MCA leading to increased EDH-type dilations to uridine 5'-triphosphate (Marrelli 2002). Therefore, further studies are required to determine whether peroxynitrite or other oxidative stress-derived molecules produced during I/R are also capable of augmenting endothelial SK_{Ca} channel relaxations by potentiating Ca^{2+} release from endothelial stores. Finally, the present study has a few technical limitations that deserve attention. First, the changes observed in an isolated human microvascular endothelial cell line do not necessarily reflect those of the endothelial layer of a rat MCA, as, for instance, the vessel source and the isolation and culture of cells affect cell phenotype and function; ~~and~~ second, in our Western blot analysis of SK_{Ca} channel expression, we were unable to detect the functional high molecular weight form of the channel, and additionally, we could not discard that SK_{Ca} channel structure/expression may differ in cultured HMVEC and intact rat MCA; and third, although we have used one of the rodent models that most closely resembles a human ischemic stroke, the disadvantages of the use of an animal stroke model should be considered (Fluri *et al.* 2015).

This article is protected by copyright. All rights reserved.

Accepted Article

Accepted Article

Cerebral artery constriction can worsen brain damage during I/R, whereas dilation can decrease cerebrovascular resistance and contribute to blood-brain barrier disruption and oedema formation (Palomares & Cipolla 2011). For example, reactive hyperaemia (i.e. CBF increases above basal levels at reperfusion) has been associated with adverse events such as increased blood-brain barrier leakage, oedema and more severe brain damage in experimental (Pérez-Asensio *et al.* 2010, Onetti *et al.* 2015) and human (Yu *et al.* 2015) ischaemic stroke. Notably, reactive hyperaemia is coupled to exacerbated protein tyrosine nitration in brain parenchyma and MCA (Pérez-Asensio *et al.* 2010, Onetti *et al.* 2015). Similarly, the greater EDH-type relaxation induced by peroxynitrite under prothrombotic conditions may contribute to decrease cerebrovascular resistance, promoting further brain damage during I/R.

In summary, we have demonstrated that the ability of TP stimulation to curtail EDH-type relaxation evoked by PAR2 signalling is absent after I/R, which reveal a novel mechanism whereby EDH may compensate loss of NO-mediated relaxation in prothrombotic disease states such as ischaemic stroke (Chamorro 2009). While this response could be considered as a key mechanism to improve regional blood flow (Golding *et al.* 2002), it might also contribute to blood-brain barrier disruption and oedema formation. We therefore propose that peroxynitrite-induced augmented EDH-type responses may constitute a previously unidentified mechanism involved in promoting neurovascular injury during I/R. The present experimental study support the use of peroxynitrite decomposing/scavenging compounds as potentially effective therapeutic strategies in the treatment of postischemic brain injury.

Conflict of interest

The authors have no conflict of interests.

This article is protected by copyright. All rights reserved.

Accepted Article

Acknowledgments

We are grateful to Prof. Gustavo Egea for helpful comments and to the confocal microscopy core from the Institut de Neurociències (Universitat Autònoma de Barcelona). This work was supported by Ministerio de Ciencia e Innovación [SAF2010-19282, SAF2014-56111-R] to E.V.; Generalitat de Catalunya [2014SGR574] to E.V. and F.J-A.; and Instituto de Salud Carlos III [FIS PI13/0091, RIC RD12/0042/0006] to AP.D. Y.O. is a predoctoral fellow of the Ministerio de Educación y Ciencia (Spain).

References

Balavoine, G.G. & Geletii, Y.V. 1999. Peroxynitrite scavenging by different antioxidants. Part I: convenient assay. *Nitric Oxide* **3**, 40–54.

Boardman, K.C., Aryal, A.M., Miller, W.M. & Waters, C.M. 2004. Actin re-distribution in response to hydrogen peroxide in airway epithelial cells. *J Cell Physiol* **199**, 57–66.

Brzezinska, A.K., Gebremedhin, D., Chilian, W.M., Kalyanaraman, B. & Elliott, S.J. 2000. Peroxynitrite reversibly inhibits Ca(2+)-activated K(+) channels in rat cerebral artery smooth muscle cells. *Am J Physiol Heart Circ Physiol* **278**, 1883–1890.

Chamorro, A. 2009. TP receptor antagonism: a new concept in atherothrombosis and stroke prevention. *Cerebrovasc Dis* **27**, 20–27.

Cipolla, M.J. 2009. The Cerebral Circulation. In: Colloquium Series on Integrated Systems Physiology: From Molecule to Function, pp. 1-59. Morgan & Claypool Life Sciences, San Rafael (CA).

This article is protected by copyright. All rights reserved.

Accepted Article

Cipolla, M.J., Smith, J., Kohlmeyer, M.M. & Godfrey, J.A. 2009. SKCa and IKCa Channels, myogenic tone, and vasodilator responses in middle cerebral arteries and parenchymal arterioles: effect of ischemia and reperfusion. *Stroke* **40**, 1451–1457.

Coucha, M., Li, W., Johnson, M.H., Fagan, S.C., Ergul, A. 2013. Protein nitration impairs the myogenic tone of rat middle cerebral arteries in both ischemic and nonischemic hemispheres after ischemic stroke. *Am J Physiol Heart Circ Physiol* **305**, 1726–1735.

Coutts, S.B. & Goyal, M. 2009. When recanalization does not improve clinical outcomes. *Stroke* **40**, 2661.

Crane, G.J. & Garland, C.J. 2004. Thromboxane receptor stimulation associated with loss of SKCa activity and reduced EDHF responses in the rat isolated mesenteric artery. *Br J Pharmacol* **142**, 43–50.

Dalle-Donne, I., Rossi, R., Milzani, A., Di Simplicio, P. & Colombo, R. 2001. The actin cytoskeleton response to oxidants: from small heat shock protein phosphorylation to changes in the redox state of actin itself. *Free Radic Biol Med* **31**, 1624–1632.

Edwards, D.H., Li, Y. & Griffith, T.M. 2008. Hydrogen peroxide potentiates the EDHF phenomenon by promoting endothelial Ca2+ mobilization. *Arterioscler Thromb Vasc Biol* **28**,1774–1781.

Ellinsworth, D.C., Shukla, N., Fleming, I. & Jeremy, J.Y. 2014. Interactions between thromboxane A_2, thromboxane/prostaglandin (TP) receptors, and endothelium-derived hyperpolarization. *Cardiovasc Res* **102**, 9–16.

Fluri, F., Schuhmann, M.K. & Kleinschnitz, C. 2015. Animal models of ischemic stroke and their application in clinical research. *Drug Des Devel Ther* **9**, 3445–3454.

This article is protected by copyright. All rights reserved.

Gauthier, K.M., Campbell, W.B. & McNeish, A.J. 2014. Regulation of KCa2.3 and endothelium-dependent hyperpolarization (EDH) in the rat middle cerebral artery: the role of lipoxygenase metabolites and isoprostanes. *PeerJ* **2**, e414.

George, P.M. & Steinberg G.K. 2015. Novel Stroke Therapeutics: Unraveling Stroke Pathophysiology and Its Impact on Clinical Treatments. *Neuron* **87**, 297–309.

Ghisdal, P., Vandenberg, G. & Morel, N. 2003. Rho-dependent kinase is involved in agonist-activated calcium entry in rat arteries. *J Physiol* **551**, 855–867.

Golding, E.M., Marrelli, S.P., You, J. & Bryan, R.M. Jr. 2002. Endothelium-derived hyperpolarizing factor in the brain: a new regulator of cerebral blood flow? *Stroke* **33**, 661–663.

Gorovoy, M., Niu, J., Bernard, O., Profirovic, J., Minhall, R., Neamu, R. & Voyno-Yasenetskaya, T. 2005. LIM kinase 1 coordinates microtubule stability and actin polymerization in human endothelial cells. *J Biol Chem* **280**, 26533–26542.

Hougaard, C., Eriksen, B.L., Jørgensen, S., Johansen, T.H., Dyhring, T., Madsen, L.S., Strøbaek, D. & Christophersen, P. 2007. Selective positive modulation of the SK3 and SK2 subtypes of small conductance Ca2+-activated K+ channels. *Br J Pharmacol* **151**, 655–665.

Hwa, J.J., Ghibaudi, L., Williams, P., Chintala, M., Zhang, R., Chatterjee, M. & Sybertz, E. 1996. Evidence for the presence of a proteinase-activated receptor distinct from the thrombin receptor in vascular endothelial cells. *Circ Res* **78**, 581–588.

Kilkenny, C., Browne, W.J. & Cuthill, I.C., Emerson, M. & Altman, D.G. 2010. Improving Bioscience Research Reporting: The ARRIVE Guidelines for Reporting Animal Research. *PLOS Biol* **8**, e1000412.

This article is protected by copyright. All rights reserved.

Accepted Article

Kojo, K.H., Higaki, T., Kutsuna, N., Yoshida, Y., Yasuhara, H. & Hasezawa, S. 2013. Roles of cortical actin microfilament patterning in division plane orientation in plants. *Plant Cell Physiol* **54**, 1491–1503.

Koo, D.D., Welsh, K.I., West, N.E., Channon, K.M., Penington, A.J., Roake, J.A., Morris, P.J. & Fuggle, S.V. 2001. Endothelial cell protection against ischemia/reperfusion injury by lecithinized superoxide dismutase. *Kidney Int* **60**, 786–796.

Koumura, A., Hamanaka, J., Kawasaki, K., Tsuruma, K., Shimazawa, M., Hozumi, I., Inuzuka, T. & Hara, H. 2011. Fasudil and ozagrel in combination show neuroprotective effects on cerebral infarction after murine middle cerebral artery occlusion. *J Pharmacol Exp Ther* **338**, 337–344.

Kunz, A., Park, L., Abe, T., Gallo, E.F., Anrather, J., Zhou, P. & Iadecola, C. 2007. Neurovascular protection by ischemic tolerance: role of nitric oxide and reactive oxygen species. *J Neurosci* **27**, 7083–7093.

Levina, N.N., Lew, R.R. & Heath, I.B. 1994. Cytoskeletal regulation of ion channel distribution in the tip-growing organism Saprolegnia ferax. *J Cell Sci* **107**, 127–134.

Li, J., Li, W., Altura, B.T. & Altura, B.M. 2005. Peroxynitrite-induced relaxation in isolated rat aortic rings and mechanisms of action. *Toxicol Appl Pharmacol* **209**, 269–276.

Liu, Y., Terata, K., Chai, Q., Li, H., Kleinman, L.H. & Gutterman, D.D. 2002. Peroxynitrite inhibits Ca2+-activated K+ channel activity in smooth muscle of human coronary arterioles. *Circ Res* **91**, 1070–1076.

Lock, J.T., Sinkins, W.G. & Schilling, W.P. 2012. Protein S-glutathionylation enhances Ca2+-induced Ca2+ release via the IP3 receptor in cultured aortic endothelial cells. *J Physiol* **590**, 3431–3447.

This article is protected by copyright. All rights reserved.

Lu, L., Timofeyev, V., Li, N., Rafizadeh, S., Singapuri, A., Harris, T.R. & Chiamvimonvat, N. 2009. Alpha-actinin2 cytoskeletal protein is required for the functional membrane localization of a Ca2+-activated K+ channel (SK2 channel). *Proc Natl Acad Sci U S A* **106**, 18402–18407.

Luykenaar, K.D., El-Rahman, R.A., Walsh, M.P. & Welsh, D.G. 2009. Rho-kinase-mediated suppression of KDR current in cerebral arteries requires an intact actin cytoskeleton. *Am J Physiol Heart Circ Physiol* **296**, 917–926.

Maneen, M.J. & Cipolla, M.J. 2007. Peroxynitrite diminishes myogenic tone in cerebral arteries: role of nitrotyrosine and F-actin. *Am J Physiol Heart Circ Physiol* **292**, 1042–1050.

Maneen, M.J., Hannah, R., Vitullo, L., DeLance, N. & Cipolla, M.J. 2006. Peroxynitrite diminishes myogenic activity and is associated with decreased vascular smooth muscle F-actin in rat posterior cerebral arteries. *Stroke* **37**, 894–899.

Marrelli, S.P. 2002. Altered endothelial Ca2+ regulation after ischemia/reperfusion produces potentiated endothelium-derived hyperpolarizing factor-mediated dilations. *Stroke* **33**, 2285–2291.

Marrelli, S.P., Khorovets, A., Johnson, T.D., Childres, W.F. & Bryan, R.M. Jr. 1999. P2 purinoceptor-mediated dilations in the rat middle cerebral artery after ischemia-reperfusion. *Am J Physiol* **276**, 33–41.

McNeish, A.J., Dora, K.A., & Garland, C.J. 2005. Possible role for K+ in endothelium-derived hyperpolarizing factor-linked dilatation in rat middle cerebral artery. *Stroke* **36**, 1526–1532.

McNeish, A.J. & Garland, C.J. 2007. Thromboxane A2 inhibition of SKCa after NO synthase block in rat middle cerebral artery. *Br J Pharmacol* **151**, 441–449.

Accepted Article

This article is protected by copyright. All rights reserved.

McNeish, A.J., Jimenez-Altayo, F., Cottrell, G.S. & Garland, C.J. 2012. Statins and selective inhibition of Rho kinase protect small conductance calcium-activated potassium channel function (K(Ca)2.3) in cerebral arteries. *PLoS One* **7**, e46735.

McNeish, A.J., Sandow, S.L., Neylon, C.B., Chen, M.X., Dora, K.A., & Garland, C.J. 2006. Evidence for involvement of both IKCa and SKCa channels in hyperpolarizing responses of the rat middle cerebral artery. *Stroke* **37**, 1277–1282.

Moldovan, L., Irani, K., Moldovan, N.I., Finkel, T. & Goldschmidt-Clermont, P.J. 1999. The actin cytoskeleton reorganization induced by Rac1 requires the production of superoxide. *Antioxid Redox Signal* **1**, 29–43.

Onetti, Y., Dantas, A.P., Pérez, B., Cugota, R., Chamorro, A., Planas, A.M., Vila, E. & Jiménez-Altayó, F. 2015. Middle cerebral artery remodeling following transient brain ischemia is linked to early postischemic hyperemia: a target of uric acid treatment. *Am J Physiol Heart Circ Physiol* **308**, 862–874.

Palomares, S.M. & Cipolla, M.J. 2011. Vascular protection following ischemia and reperfusion. *J Neurol Neurophysiol* **20**, S1–004.

Pérez-Asensio, F.J., de la Rosa, X., Jiménez-Altayó, F., Gorina, R., Martínez, E., Messeguer, A., Vila, E., Chamorro, A. & Planas, A.M. 2010. Antioxidant CR-6 protects against reperfusion injury after a transient episode of focal brain ischemia in rats. *J Cereb Blood Flow Metab* **30**, 638–652.

Plane, F. & Garland, C.J. 1996. Influence of contractile agonists on the mechanism of endothelium-dependent relaxation in rat isolated mesenteric artery. *Br J Pharmacol* **119**, 191–193.

Prasain, N. & Stevens, T. 2009. The actin cytoskeleton in endothelial cell phenotypes. *Microvasc Res* **77**, 53–63.

This article is protected by copyright. All rights reserved.

Accepted Article

Accepted Article

Rafizadeh, S., Zhang, Z., Woltz, R.L., Kim, H.J., Myers, R.E., Lu, L., Tuteja, D., Singapuri, A., Bigdeli, A.A., Harchache, S.B., Knowlton, A.A., Yarov-Yarovoy, V., Yamoah, E.N. & Chiamvimonvat, N. 2014. Functional interaction with filamin A and intracellular Ca2+ enhance the surface membrane expression of a small-conductance Ca2+-activated K+ (SK2) channel. *Proc Natl Acad Sci U S A*, **111**, 9989–9994.

Smeda, J.S. & McGuire, J.J. 2007. Effects of poststroke Losartan versus Captopril treatment on myogenic and endothelial function in the cerebrovasculature of SHRsp. *Stroke* **38**, 1590–1596.

Spector, I., Shochet, N.R., Blasberger, D. & Kashman, Y. 1989. Latrunculins--novel marine macrolides that disrupt microfilament organization and affect cell growth: I. Comparison with cytochalasin D. *Cell Motil Cytoskeleton* **13**, 127–144.

Wakatsuki, T., Schwab, B., Thompson, N.C. & Elson, E.L. 2001. Effects of cytochalasin D and latrunculin B on mechanical properties of cells. *J Cell Sci* **114**, 1025–1036.

Yasmin, W., Strynadka, K.D. & Schulz, R. 1997. Generation of peroxynitrite contributes to ischemia-reperfusion injury in isolated rat hearts. *Cardiovasc Res* **33**, 422–432.

Yu, S., Liebeskind, D.S., Dua, S., Wilhalme, H., Elashoff, D., Qiao, X.J., Alger, J.R., Sanossian, N., Starkman, S., Ali, L.K., Scalzo, F., Lou, X., Yoo, B., Saver, J.L., Salamon, N. & Wang, D.J. *et al*. 2015. Postischemic hyperperfusion on arterial spin labeled perfusion MRI is linked to hemorrhagic transformation in stroke. *J Cereb Blood Flow Metab* **35**, 630–637.

This article is protected by copyright. All rights reserved.

Legends to figures

Figure 1. Relaxation to SLIGRL (20 μmol L^{-1}) in U46619 (30-100 nmol L^{-1})-preconstricted MCA from sham and ischemia/reperfusion (I/R) rats in the presence of l-NAME (300 μmol L^{-1}) and indomethacin (10 μmol L^{-1}) to isolate EDH-type relaxation in (a) sham and ipsilateral (ipsi) or contralateral (contra) to I/R arteries and (b) ipsilateral arteries in the absence and presence of the IK_{Ca} channel blocker TRAM-34 (1 μmol L^{-1}) or the SK_{Ca} channel blocker apamin (100 nmol L^{-1}), alone or in combination. (c) Representative tracings showing the isolated EDH-type responses evoked by SLIGRL in sham and I/R arteries. Data are shown as mean ± SEM from 13 sham, 9 ipsilateral I/R and 8 contralateral I/R arteries (a) or 12 sham control, 5 sham + TRAM-34, 5 sham + apamin, 6 sham + TRAM-34 + apamin, 8 I/R control, 8 I/R + TRAM-34, 3 I/R + apamin and 7 I/R + TRAM-34 + apamin arteries (b) of different animals. *P < 0.05; **P < 0.01 vs. sham; $^{\dagger}P$ < 0.05, $^{\dagger\dagger}P$ < 0.01, $^{\dagger\dagger\dagger}P$ < 0.001 vs. control; $^{\ddagger\ddagger}P$ < 0.01 vs. TRAM-34, by one (a) or two (b)-way ANOVA with Tukey's post-test.

Figure 2. Protein expression in an endothelial cell model of hypoxia/reoxygenation (H/R). (a) Western blot and densitometric analyses (bottom), normalized to the expression of GAPDH, of hypoxia-inducible factor 1α (HIF-1α) expression and (b) pull-down assay (immunoblot) of Rho-mediated signal activation and densitometric analyses (bottom), normalized to total RhoA, in human microvascular endothelial cells exposed to H/R in the absence and presence of U46619 (100 nmol L^{-1}). Data are shown as mean ± SEM from 6 independent experiments obtained in two batches of cells at different passages. ***P < 0.001 vs. control by Student's *t*-test (a); *P < 0.05, ***P < 0.001 vs. non-treated or $^{\dagger\dagger}P$ < 0.01 vs. control + U46619 by two-way ANOVA with Tukey's post-test (b).

This article is protected by copyright. All rights reserved.

Figure 3. SK_{Ca} channel expression. (a) Western blot and densitometric analyses (bottom), normalized to the expression of GAPDH, of SK_{Ca} channel expression in human microvascular endothelial cells exposed to hypoxia/reoxygenation (H/R) in the absence and presence of U46619 (100 nmol L^{-1}). Data are shown as mean ± SEM from 6 independent experiments obtained in two batches of cells at different passages. (b) Representative photomicrographs of SK_{Ca} channel immunofluorescence (red) of confocal microscopic sections of human microvascular endothelial cells exposed to H/R (*n* = 4 independent experiments obtained in two batches of cells at different passages). Filamentous (F)-actin staining (green) is also shown. (c) Representative photomicrographs of SK_{Ca} channel immunofluorescence (red) of confocal microscopic MCA sections of rats submitted to ischemia/reperfusion (I/R; *n* = 4 arteries of different animals per group). Natural autofluorescence of elastin (green) and nuclear staining (blue) are also shown. EC, endothelial cell; AC, adventitial cell.

Figure 4. Analysis of endothelial cell actin expression. (a) Representative photomicrographs of filamentous (F)- (red) and globular (G)-actin (green) immunofluorescence of confocal microscopic sections and (b) immunoblot and densitometric analyses (right) of F- relative to G-actin expression in human microvascular endothelial cells exposed to hypoxia/reoxygenation (H/R) or peroxynitrite ($ONOO^-$; 500 nmol L^{-1}). Nuclear staining (blue) is also shown. Data are shown as mean ± SEM from 4-6 independent experiments obtained in two batches of cells at different passages. ***$P < 0.001$ vs. control non-treated by one-way ANOVA with Tukey's post-test. (c) Representative raw (left) and mask (right) 3D reconstructions and quantification of F-actin fluorescence (red) in confocal microscopic intact MCA stacks of serial optical slices of the endothelial layer of rats submitted to ischemia/reperfusion (I/R) or non-operated (control) rats incubated with cytochalasin D (CytD; 50 nmol L^{-1}) or $ONOO^-$ (5 µmol L^{-1}). Nuclear staining (blue) is also shown. Cuboid regions of interest are marked with a dotted white line. EC, endothelial cell; SMC, smooth

This article is protected by copyright. All rights reserved.

Accepted Article

muscle cell. Data are shown as mean ± SEM from 4 sham, 3 I/R, 4 control + CytD and 4 control + $ONOO^-$ arteries of different animals. *P < 0.05 vs. sham by one-way ANOVA with Tukey's post-test.

Figure 5. Effect of incubation with actin cytoskeleton-disrupting agents on endothelium-dependent relaxation in U46619 (30-100 nmol L^{-1})-preconstricted MCA from non-operated (control) rats in the presence of l-NAME (300 µmol L^{-1}) and indomethacin (10 µmol L^{-1}) to isolate EDH-type relaxation. (a) Concentration-dependent effects of latrunculin B (10 nmol L^{-1}-1 µmol L^{-1}) on SLIGRL (20 µmol L^{-1}) relaxation. (b) Effects of cytochalasin D (CytD; 50 nmol L^{-1}) on SLIGRL relaxation in the absence and presence of TRAM-34 (1 µmol L^{-1}) or apamin (100 nmol L^{-1}), alone or in combination. (c) Representative tracings (upper panels) and analysis (bottom panel) of SK_{Ca} channel-mediated relaxation induced by the selective SK_{Ca} channel activator CyPPA (100 µmol L^{-1}) in control or CytD-incubated arteries in the absence and presence of apamin. Data are shown as mean ± SEM from 6 control, 6 control + latrunculin B (10 nmol L^{-1}), 5 control + latrunculin B (100 nmol L^{-1}) and 5 control + latrunculin B (1 µmol L^{-1}) (a) or 8 control, 5 control + CytD, 6 control + CytD + TRAM-34, 5 control + CytD + apamin and 6 control + CytD + TRAM-34 + apamin (b) or 10 control, 7 control + apamin, 7 control + CytD and 8 control + CytD + apamin (c) arteries of different animals. *P < 0.05, **P < 0.01 vs. control; $^{\dagger\dagger}P$ < 0.01, $^{\dagger\dagger\dagger}P$ < 0.001 vs. control + CytD by one-way ANOVA with Tukey's post-test.

Figure 6. Detection of protein tyrosine nitration. (a) Representative photomicrographs and quantification of nitrotyrosine immunofluorescence (red) of confocal microscopic sections and (b) Western blot and densitometric analyses (bottom), normalized to the expression of GAPDH, of nitrotyrosine expression in human microvascular endothelial cells exposed to hypoxia/reoxygenation (H/R) or peroxynitrite ($ONOO^-$; 500 nmol L^{-1}). Filamentous (F)-actin

This article is protected by copyright. All rights reserved.

Accepted Article

(green) and nuclear staining (blue) are also shown. Representative examples of elevated nitrotyrosine immunofluorescence are indicated with arrows. Data are shown as mean ± SEM from 6 independent experiments obtained in two batches of cells at different passages. ***P < 0.001 vs. control by one-way ANOVA with Tukey's post-test. (c) Representative photomicrographs of nitrotyrosine immunofluorescence (red) of confocal microscopic MCA sections of rats submitted to ischemia/reperfusion (I/R) or MCA of non-operated (control) rats incubated with $ONOO^-$ (5 μmol L^{-1}; n = 3 arteries of different animals per group). Natural autofluorescence of elastin (green) and nuclear staining (blue) are also shown. Nitro, nitrotyrosine; EC, endothelial cell.

Figure 7. Effect of peroxynitrite ($ONOO^-$; 5 μmol L^{-1}) on endothelium-dependent relaxation in U46619 (30-100 nmol L^{-1})-preconstricted MCA from non-operated (control) rats (a, b, c) or from sham and ischemia/reperfusion (I/R) rats (d, e) in the presence of l-NAME (300 μmol L^{-1}) and indomethacin (10 μmol L^{-1}) to isolate EDH-type relaxation. (a) Effects of $ONOO^-$ on SLIGRL (20 μmol L^{-1}) relaxation in the presence of the oxidation/nitration blocker epicatechin (EPICAT; 1 μmol L^{-1}) or the actin filament stabilizer jasplakinolide (JASPK; 100 nmol L^{-1}). The effect of decomposed $ONOO^-$ (DC-$ONOO^-$; 5 μmol L^{-1}) is also shown. (b) Effects of $ONOO^-$ on SLIGRL relaxation in the absence and presence of TRAM-34 (1 μmol L^{-1}) or apamin (100 nmol L^{-1}), alone or in combination. (c) Representative tracings (upper panels) and analysis (bottom panel) of SK_{Ca} channel-mediated relaxation induced by CyPPA (100 μmol L^{-1}) in control, $ONOO^-$ or DC-$ONOO^-$-incubated arteries. (d) Effect of *in vivo* treatment with the $ONOO^-$ decomposition catalyst FeTPPS (20 mg kg^{-1}) on SLIGRL-evoked EDH-type relaxation in the absence and presence of TRAM-34 or TRAM-34 plus apamin. (e) Effect of *in vivo* treatment with FeTPPS on SK_{Ca} channel-mediated relaxation to CyPPA in the absence and presence of apamin. Data are shown as mean ± SEM from 7 control, 7 control + $ONOO^-$, 4 control + DC-$ONOO^-$, 6 control + $ONOO^-$ + EPICAT and 5 control + $ONOO^-$ + JASPK (a) or 6 control, 6 control + $ONOO^-$, 5 control + $ONOO^-$ + TRAM-34, 6 control +

This article is protected by copyright. All rights reserved.

$ONOO^-$ + apamin and 4 control + $ONOO^-$ + TRAM-34 + apamin (b) or 9 control, 7 control + $ONOO^-$ and 3 control + DC-$ONOO^-$ (c) or 7 sham + vehicle control, 7 sham + vehicle + TRAM-34, 5 sham + vehicle + TRAM-34 + apamin, 7 I/R + vehicle control, 5 I/R + vehicle + TRAM-34, 5 I/R + vehicle + TRAM-34 + apamin, 7 I/R + FeTPPS control, 6 I/R + FeTPPS + TRAM-34 and 7 I/R + FeTPPS + TRAM-34 + apamin (d) or 8 sham + vehicle, 6 I/R + vehicle, 3 I/R + vehicle + apamin and 5 I/R + FeTPPS (e) arteries of different animals. $^{**}P < 0.01$ vs. control or vs. sham + vehicle; $^{\dagger}P < 0.05$, $^{\dagger\dagger}P < 0.01$, $^{\dagger\dagger\dagger}P < 0.001$ vs. control + $ONOO^-$ or vs. non-treated; $^{\#}P < 0.05$, $^{\#\#}P < 0.01$ vs. I/R + vehicle; $^{\ddagger}P < 0.05$; $^{\ddagger\ddagger\ddagger}P < 0.001$ vs. control + $ONOO^-$ + TRAM-34 or vs. I/R + vehicle + TRAM-34, by one (a, b, c, e) or two (d)-way ANOVA with Tukey's post-test.

Supporting Information

Additional Supporting Information may be found online in the supporting information tab for this article:

Table S1. Differences (Δ) in basal tone measured before and after (30 min) addition of drugs.

Table S2. Body weight, body temperature and percentage changes in cortical cerebral blood flow (CBF), with respect to basal values, in rats submitted to ischemia (90 min)/reperfusion (24 h) (I/R) and treated with 5,10,15,20-tetrakis(4-sulfonatophenyl)prophyrinato iron (III) (FeTPPS) or vehicle.

Figure S1. Concentration-dependent relaxation to bradykinin in U46619 (30-100 nmol L^{-1})-preconstricted MCA from sham and ischemia/reperfusion (I/R) rats in the presence of l-NAME (300 μmol L^{-1}) and indomethacin (10 μmol L^{-1}) to isolate endothelium-derived hyperpolarization-type response. Data are shown as mean ± SEM from 8 sham and 6 I/R arteries of different animals

This article is protected by copyright. All rights reserved.

Accepted Article

Figure S2. Representative hypoxia-inducible factor 1α (HIF-1α) Western blot results in human microvascular endothelial cells exposed to hypoxia/reoxygenation (H/R) or peroxynitrite ($ONOO^-$; 500 nmol L^{-1}).

Figure S3. Representative SK_{Ca} channel Western blot results in human microvascular endothelial cells exposed to hypoxia/reoxygenation (H/R) in the absence and presence of U46619 (100 nmol L^{-1}).

Figure S4. Representative nitrotyrosine Western blot results in human microvascular endothelial cells exposed to hypoxia/reoxygenation (H/R) or peroxynitrite (ONOO-; 500 nmol L^{-1}).

Figure S5. Spectrophotometric analysis of peroxynitrite (2 µmol L^{-1}) oxidant activity and its decay after decomposition. Consumption of pyrogallol red (6 µmol L^{-1}) by peroxynitrite, submitted or not to different conditions, was evaluated in the presence of diphenyl diselenide. Data are shown as mean ± SEM from 3 independent experiments per group. *P < 0.05 vs. no degradation, by two-way ANOVA.

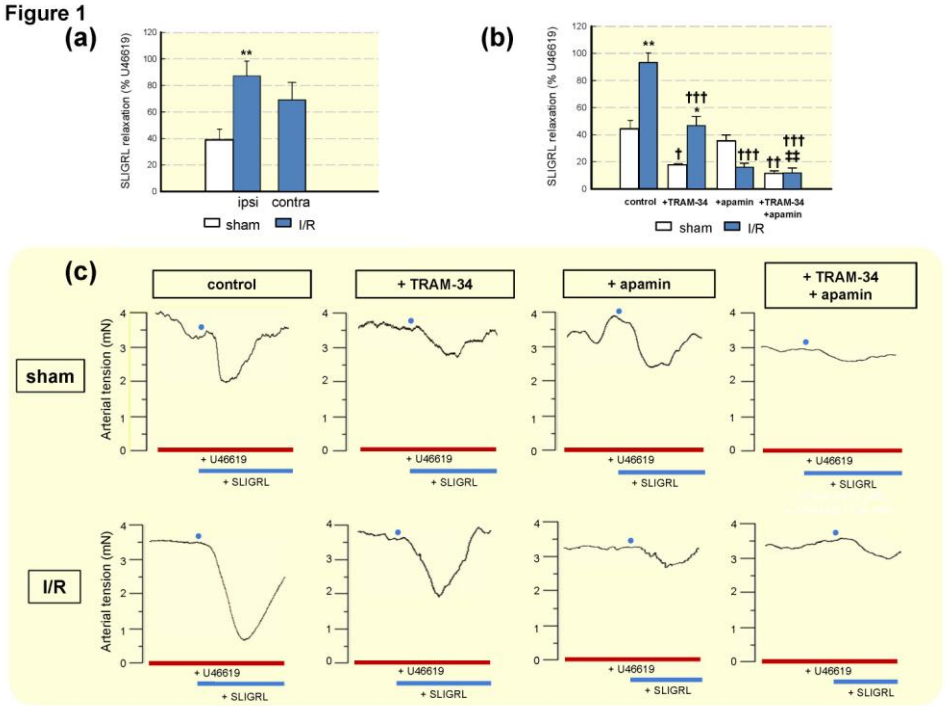

This article is protected by copyright. All rights reserved.

Accepted Article

Figure 2

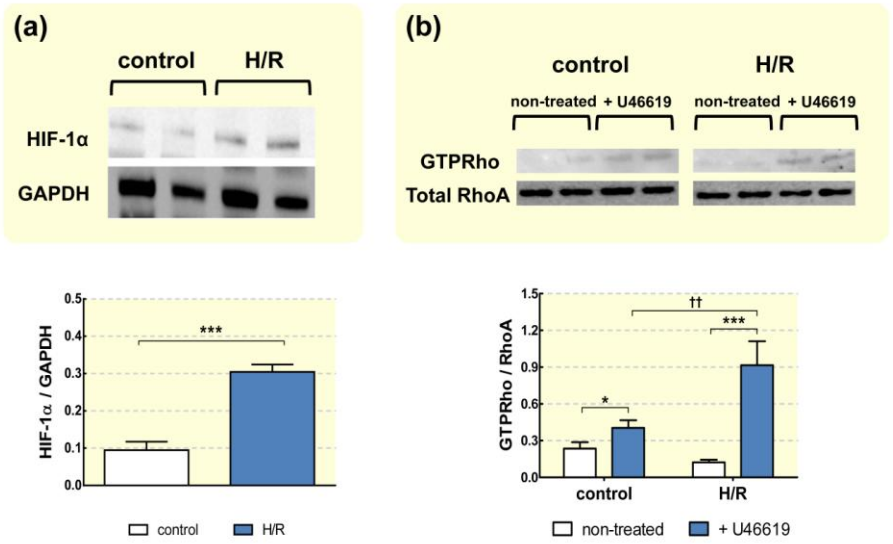

Figure 3

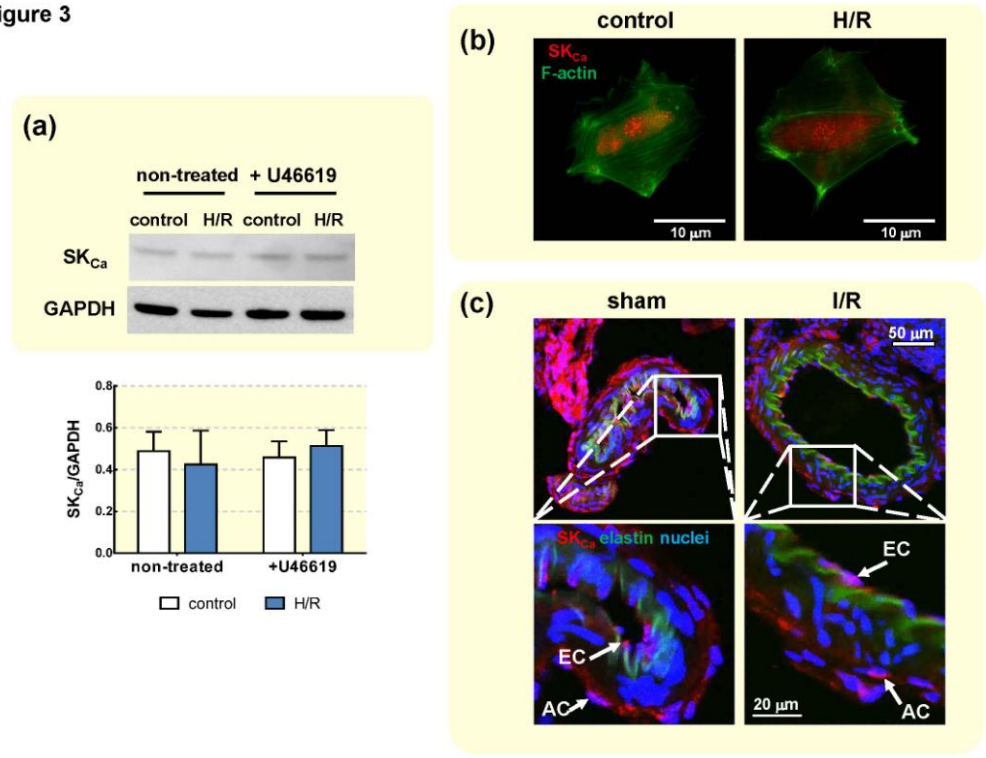

This article is protected by copyright. All rights reserved.

Accepted Article

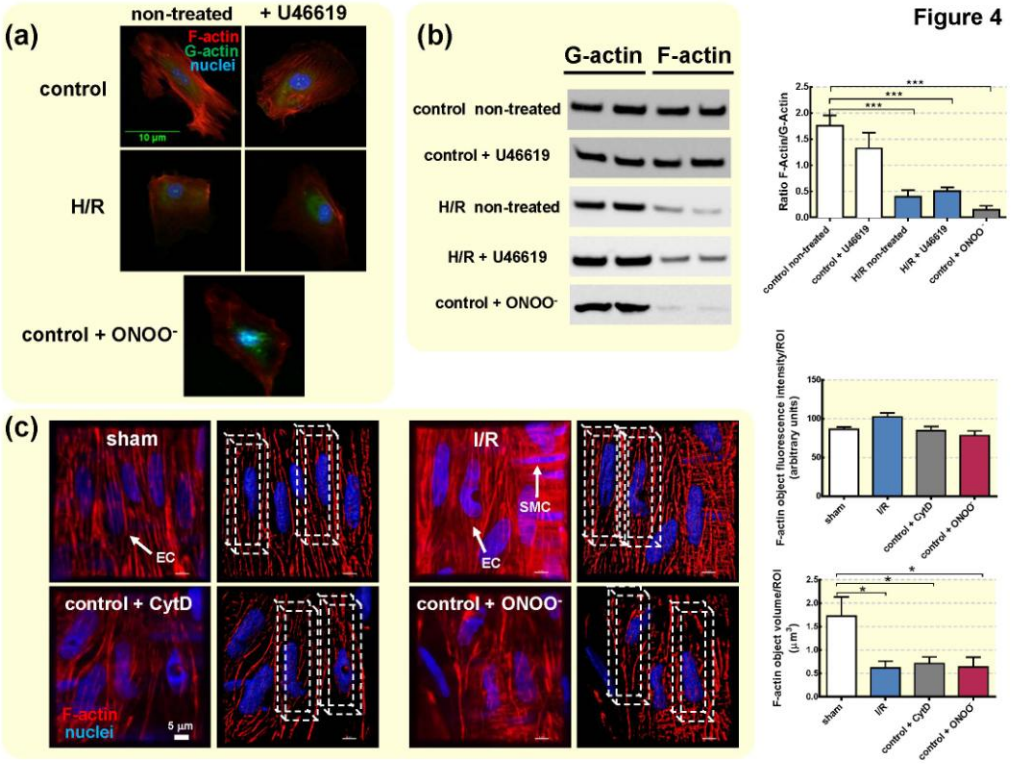

Figure 4

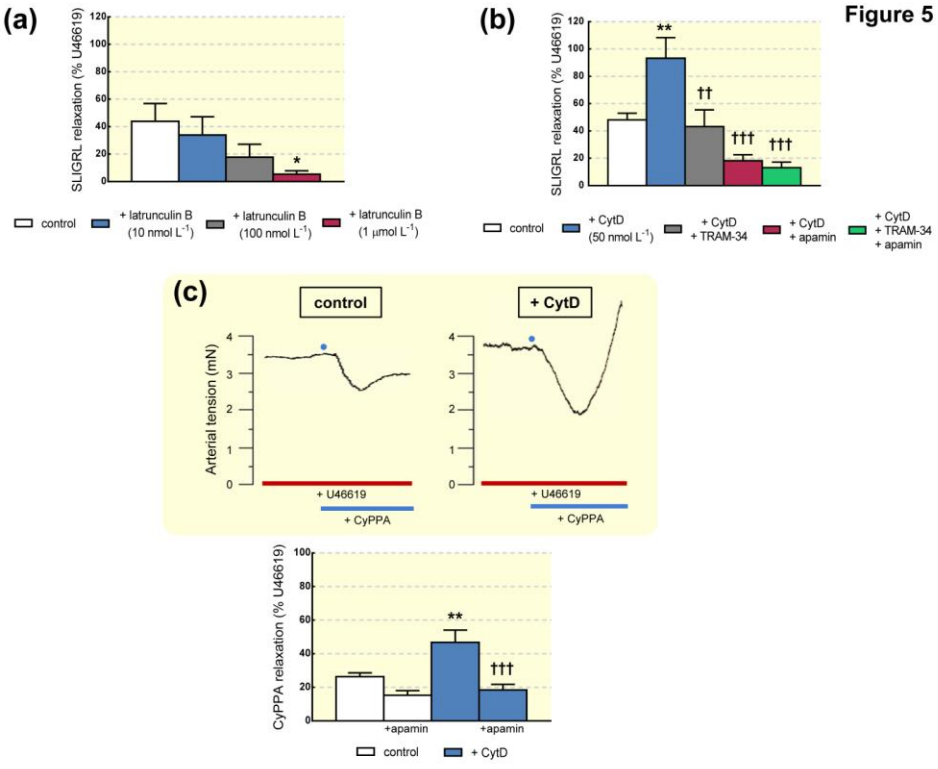

Figure 5

This article is protected by copyright. All rights reserved.

Accepted Article

Figure 6

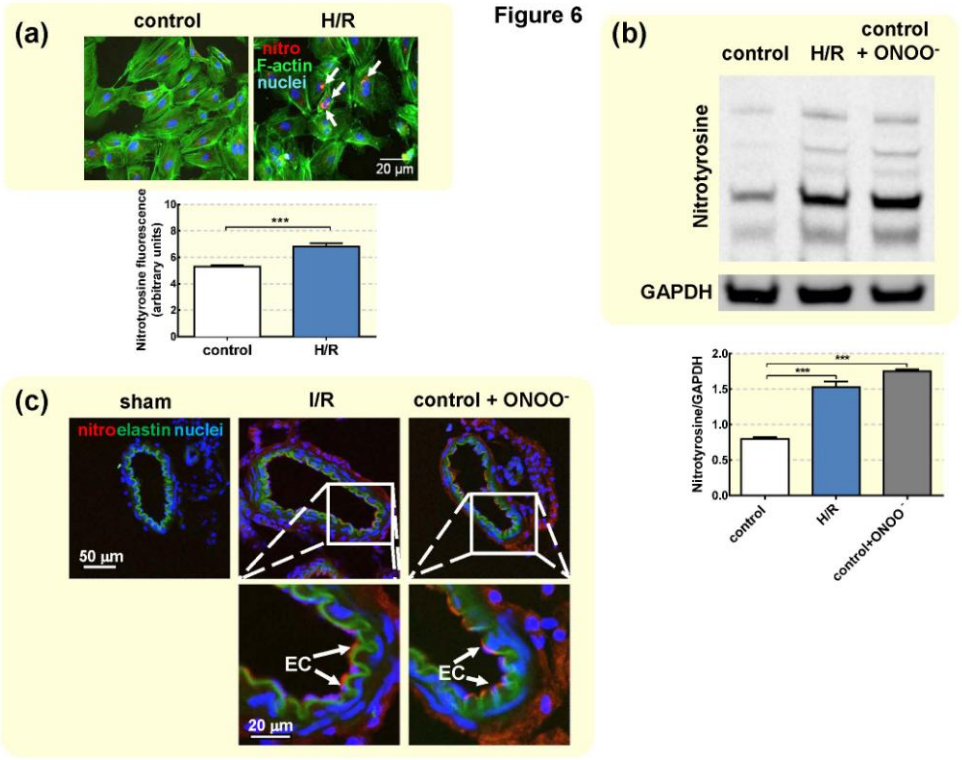

Figure 7

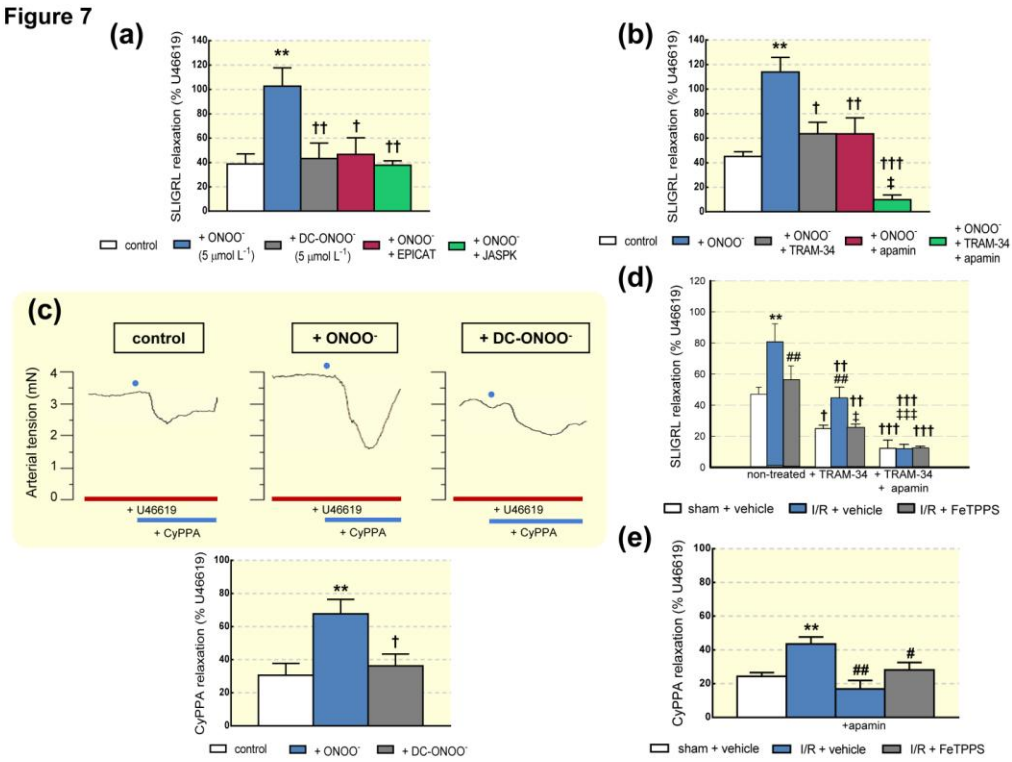

This article is protected by copyright. All rights reserved.